Nat. Hazards Earth Syst. Sci. Discuss., 1, 323–352, 2013
www.nat-hazards-earth-syst-sci-discuss.net/1/323/2013/
doi:10.5194/nhessd-1-323-2013
© Author(s) 2013. CC Attribution 3.0 License.

Natural Hazards and Earth System Sciences
Open Access
Discussions

This discussion paper is/has been under review for the journal Natural Hazards and Earth System Sciences (NHESS). Please refer to the corresponding final paper in NHESS if available.

# Seismicity in northeast edge of the Mexican Volcanic Belt (MVB), activation of an undocumented fault: the Peñamiller earthquake sequence of 2011, Queretaro, Mexico

**A. Clemente-Chavez[1], A. Figueroa-Soto[2], F. R. Zúñiga[2], M. Arroyo[1], M. Montiel[1], and O. Chavez[1]**

[1]División de Investigación y Posgrado, Facultad de Ingeniería, Universidad Autónoma de Querétaro, Centro Universitario, Cerro de las Campanas s/n, Querétaro, Querétaro, C.P. 76010, México
[2]Centro de Geociencias (CGEO), Juriquilla, UNAM, P.O. Box 1-742, Querétaro, Querétaro, C.P. 76001, México

Received: 11 January 2013 – Accepted: 3 February 2013 – Published: 21 February 2013

Correspondence to: A. Clemente-Chavez (aclemente09@alumnos.uaq.mx)

Published by Copernicus Publications on behalf of the European Geosciences Union.

## Abstract

~~The~~ Peñamiller town, in the Queretaro ~~state,~~ Mexico is located at the northeast border of the seismogenic zone known as the Mexican Volcanic Belt (MVB), which covers a central ~~fringe~~ of Mexico ~~with~~ east-west orientation. In this town, a sequence of small earthquakes occurred during the end of 2010 and beginning of 2011. Seismicity ~~frequent~~ in ~~of~~ the continental regimen of central Mexico ~~are~~ not common, however, it is known that there are precedents of large earthquakes ($M_w$ magnitude greater than 6.0) occurring in this zone. ~~In order~~ to ~~enrich~~ seismic information, which has not been analyzed ~~nor~~ documented ~~until this moment, is presented this work.~~ This will contribute to ~~gain more insight into~~ the tectonic situation of the central Mexico region.

Twenty-four shallow earthquakes ~~records~~ of the Peñamiller, Queretaro seismic sequence of 2011 were recorded by a provisional accelerograph network from the Universidad Autonoma de Queretaro (UAQ). The data were analysed in order to determine the source locations and ~~for the estimation of~~ the source parameters. The study was carried out through an inversion process and by spectral analysis. The results show that the largest earthquake~~,~~ occurred on 8 February 2011 at 19:53:48.6 UTC, had a moment magnitude $M_w = 3.5$, and was located at latitude 21.039° and longitude −99.752°, at a depth of 5.6 km. This zone is located less than 7 km away in south-east direction from downtown Peñamiller. The focal mechanisms are mostly normal faults with ~~a~~ small lateral component~~.~~ ~~This feature is~~ consistent with the extensional regimen of the southern extension of the Basin and Range (BR) province. The source area of the largest event was estimated to have a radius of 0.5 km, which corresponds to a normal fault with azimuth of 174° and an almost pure dip slip; this caused ~~Peak~~ Ground Acceleration (PGA) of up to 100 cm s$^{-2}$ in the horizontal direction. It is evident that the shallow earthquakes induced by crustal faulting can present a potential seismic risk and hazard within the MVB and considering the population growth, the necessity to enrich seismic information in this zone is very important; which at most urban sites in the region might even be greater than the risk posed by subduction earthquakes.






NHESSD
1, 323–352, 2013



CC BY

## 1 Introduction

~~The~~ Peñamiller town, in the Mexican provi~~nce~~ of Queretaro, is located at the northeast border of the seismogenic zone known as the MVB, which ~~covers~~ a central ~~fringe~~ of Mexico with east-west orientation, between the geographical coordinates 19° and 22° north latitude and 96° and 106° west longitude. The MVB is mostly a calc-alkaline volcanic arc which was formed as a result of subduction of the Rivera and Cocos plate underneath the North American plate (Suter, 1991).

The regional tectonic situation of the MVB is shown in Fig. 1. The central zone of the MVB includes several ~~Faults Systems~~ such ~~known~~ as: Chapala-Tula (CTFS) (Johnson and Harrison, 1990); Morelia-Acambay (MAFS) (Martínez-Reyes and Nieto-Samaniego, 1990; Pasquaré et al., 1988); and Bajío (BFS) (Nieto-Samaniego et al., 1999; Alaniz-Álvarez and Nieto-Samaniego, 2005). This arc-parallel fault zone, and the volcanic arc itself, are superposed on a nearly perpendicular preexisting stress and deformation province, which may correspond to the extension of the ~~BR~~ into Mexico (Suter, 1991). The BR province comprises north-northwest to north-northeast-striking normal faults, some of these faults are grouped in the Taxco-San Miguel Allende Fault Systems (TSMFS) (Demant, 1978; Pasquaré et al., 1987; Nixon et al., 1987). An example of the activity of this system was provided by the seismic sequence of Sanfandila, Queretaro, in 1998, reported by Zúñiga et al. (2003). The orientation of major faults in the TSMFS zone was identified through satellite and aerial imagery analyzed by Aguirre-Díaz et al. (2005).

The western zone of the MVB includes several ~~Faults Systems~~ such as: Chapala (CHFS) defined as two half-graben of opposite convergence (Urrutia-Fucugauchi and Rosas-Elguera, 1994; Rosas-Elguera and Urrutia-Fucugauchi, 1998); Tepic-Zacoalco (TZFS), Colima (CFS) and Chapala (CHFS), intersecting at a triple joint to the south of Guadalajara (Demant, 1981).

The eastern zone of the MVB includes ~~Faults Systems~~ such as: Pera-Tenango (PTFS) ~~with east-west orientation~~ (García-Palomo et al., 2000; Ferrari et al.,





NHESSD
1, 323–352, 2013



CC BY

2003); Aljibes (ALFS) and Mezquital (MZFS) with east-west orientations (Suter et al., 2001).

The stress state of the MVB zone has been inferred largely by major structures such as alignments of faults, shield volcanoes, dikes and elongations (e.g. Suter et al., 1995), mainly due to lack of seismic information because low frequency of seismic occurrence (Zúñiga et al., 2003). This lack of information ~~difficults the estimation of~~ the hazard of possible damaging earthquakes ($M_w$ magnitude greater than 6.0), such as those that have occurred within the MVB zone (e.g. Suter et al., 1996 and Zúñiga et al., 2003).

The historical seismicity in the MVB area shows that large earthquakes (see Fig. 1) can occur at depths less than 20 km (e.g. Suter et al., 1996; Zúñiga et al., 2003) with diverse ~~faults~~ styles. However, the most common fault type is extensional with north-south direction (Zúñiga et al., 2003). In general, the MVB regional tectonics is characterized as extensional type with north-south direction (Suter et al., 2001), although other orientations have been shown in some central parts of Mexico (Suter et al., 1995; Alaniz-Alvarez et al., 1998; Zúñiga et al., 2003).

In order to ~~enrich~~ seismic information for this type of faulting to gain more insight into the tectonic situation ~~and of the~~ seismic risk of the region, ~~such as occur in others world regions~~ (e.g. Polonia et al., 2012; Vipin et al., 2009; Del Gaudio et al., 2009). In this ~~work is carried~~ out a detailed analysis of the seismic source parameters of events of the Peñamiller sequence, monitored during the first three months of 2011.

### 1.1 The Peñamiller seismic sequence

The sequence of small earthquakes ($M_w < 4.0$) took place near the town of Peñamiller, in the state of Queretaro, at the end of 2010 and beginning of 2011. Peñamiller is located between the geographical coordinates 20°57′ and 21°14′ north latitude and 99°42′ and 100°02′ west longitude, ~~at~~ the foothills of the Sierra Gorda, about 80 km northeast of ~~the~~ Queretaro ~~c~~ity. As a result of reports of earthquakes that caused consternation in the local communities, a small seismic network consisting of three accelerographs was provisionally installed by the UAQ. The first part of the study





NHESSD
1, 323–352, 2013



CC BY

consisted ~~on the identification of~~ the origin of the activity and ~~the estimation of~~ seismic source parameters, in order to analyze and associate its occurrence with the regional tectonic regime of the MVB.

Additionally, this paper also presents other important information such as PGA. This information has not been ~~shown~~ for local earthquakes in the northeastern region of MVB, and will help to contrast the vulnerability of population in the region to local seismic hazard sources with ~~respect to that caused by~~ the occurrence of large regional events. All results are presented and discussed in detail below.

## 2 Data analysis

A total of 24 accelerograms from 8 events were analyzed for the characterization of the Peñamiller Earthquake Sequence (PES), see Table 1. The three seismic stations were installed near the town of Peñamiller, at distances from 4 to 16 km; in two of the stations Etna accelerographs were installed, ~~using~~ a K2 model in the third station (both models are Kinemetrics line). The station locations were ~~defined according to the~~ intensity reports from the local population, the safety of equipment and ~~to~~ provide good azimuthal coverage. The stations were located at three communities, whose names were associated with each ~~station; so stations are~~ Extoraz (EXT1), Pilon (PIL1), Higuerillas (HIG1, later renamed as HIG2, when it was relocated) and Peñamiller Town Center (PEN2). All stations are shown in Fig. 2.

### 2.1 Seismic location

SEISAN software package (Havskov and Ottemoller, 2000) was used to locate the events, ~~including~~ a crustal velocity model shown in Table 2, which was a modified version of Zúñiga et al. (2003) following the model determined by Fuentes (1997). It was deduced from surface wave dispersion of Rayleigh waves across the MVB. The location~~s~~ results are shown in Table 3, which indicates that the events occurred at





NHESSD
1, 323–352, 2013



CC BY

depths around 5 km and between 4 to 10 km from downtown Peñamiller in a southeast direction (see Fig. 3). Table 3 also shows small error values (less than 1.34 km and rms of 0.07 s).

## 2.2 Source parameters

To estimate the source parameters of the events, ISOLA software (Sokos and Zahradnik, 2008) was used. This program employs waveform modeling (inversion) to determine the focal mechanism and the scalar seismic moment. ISOLA software is based on multiple point-source representation and iterative deconvolution method, similar to Kikuchi and Kanamori (1991) for teleseismic records, but here the full wavefield is considered, and Green's functions are calculated by the discrete wavenumber method of Bouchon (1981). Thus the method is applicable for regional and local events (Sokos and Zahradnik, 2008). The code transforms velocity into displacement, inverts the displacement, and provides synthetic displacement (Sokos and Zahradnik, 2008).

An inversion on eight events of Table 3 was performed. The results are shown in Table 4 and Fig. 3, where the largest earthquake analyzed had $M_w = 3.5$ and occurred on 8 February at 19:53:48.6 UTC, although it is possible that a larger event ($M_w > 3.5$) in the episode was missed because it occurred before the network was installed.

The lineaments of the geomorphological features from around the epicentral area and all the focal mechanisms are shown in Fig. 3a, where there is a strike tendency in the ~~South-East~~ direction; this can be seen from the average values shown in Table 4. The fault associated to the largest shock has a strike of 174°, dip of 77° and rake of −85°. In general, the results of the focal mechanisms are mostly normal faults (see Fig. 3a and discussion) with a small lateral component. This is consistent with the main trend of the southern extension of the BR (Henry and Aranda-Gómez, 1992; Suter, 1991).

The waveform modeling was done on the *P* wave phase in its three components EW, NS and V. A band-pass filter between 0.35 Hz to 4.5 Hz was applied to obtain displacement, since it was desired that the focal parameters be retrieved from the low frequency





NHESSD
1, 323–352, 2013



CC BY

signal of the records, eliminating the noise produced by high frequency scatter waves and unknown crustal structure details (Zúñiga et al., 2003).

Figure 4 shows the observed *P* wave and best fitting synthetic records obtained after the inversion for the largest event.

### 2.2.1 Spectral analysis

A spectral analysis on the seismic signal from the largest earthquake of the sequence was performed. This was done for P-wave and S-wave phases ~~for separate~~ (~~see~~ Figs. 5 and 6). In order to do it, the acceleration was integrated two times to obtain displacement. The velocity signal is shown in Fig. 5, where it can be seen that ~~did not need a special correction of base line~~. The purpose of this analysis was to estimate some source parameters ~~because~~ the inversion procedure does not take into account such as fault radius (a), stress drop ($\Delta\sigma$) besides ~~of~~ the moment magnitude ($M_w$). A correction for attenuation was ~~done~~ to the displacement spectrum to obtain correct source parameters. The attenuation values used in the correction were $k = 0.02$ (Singh et al., 1990) and $Q(f) = 98f^{0.72}$ (Singh et al., 2007); the first value correspond to the contribution on near surface attenuation and second value to the attenuation along the path. The attenuation values are the be[illegible]hoice to represent the MVB zone, since, at present, no values have been deduced from the shallow seismicity within MVB. Howeve[illegible]r this type of study (short distance and high frequencies) the near surface attenuation is important only because this is what dominates the spectral decay and in order to obtain a correct corner frequency ($f_o$) (~~see~~ Fig. 6). Figure 6 the shape of the theoretical source spectra was plotted for the displacement, according to the Brune (1970) model, thus allowing the identification of the correct spectral flat level ($\Omega o$). In addition, a plot from the spectra of background noise signal was ~~done~~ to compare with the spectra of the seismic signal. A good signal/noise ratio can be observed in ~~this figure~~ (furthe[illegible]gh >1), enough to estimate a correct $f_o$.

The results of spectral analysis are shown in Table 5. The first analysis was done based on P-window of the corrected displacement spectrum (~~see~~ Fig. 6a), where ~~a~~





NHESSD
1, 323–352, 2013



CC BY

$f_o$ = 6.0 Hz and $\Omega o = 3.03 \times 10^{-6}$ m s and consequently, values of $a$ = 516 km, $\Delta\sigma$ = 5.1 bar and $M_w$ = 3.4 were calculated. The result of $M_w$ obtained through the inversion from that from the spectral analysis were similar, $M_w$ = 3.5 and $M_w$ = 3.4, respectively. Hence, ~~it means that~~ the source area of the largest event was estimated to have a radius of 0.516 km. ~~On the other hand,~~ an analogous second analysis ~~was done with~~ the S-window (~~see~~ Fig. 6b)~~.~~ ~~However, this shown a sub estimation at~~ the magnitude of $M_w$ = 2.9 in comparison to $M_w$ = 3.5 (from inversion) and 3.4 (from P-window)~~, this~~ is because spectral flat level was not clearly ~~to~~ identified due to strong ascending line of amplitude at low frequencies ($f$ < 1 Hz) and to an amplitude drop around 2 Hz (~~see~~ Fig. 6b).

## 3 Discussion

### 3.1 Relation with regional tectonics

The statistical analysis of the $\sigma_1$ and $\sigma_3$ stress axes (the maximum and minimum compressive principal stress axes, respectively) through rose histograms (~~see~~ Table 6 and Fig. 7), taking into account all the focal mechanisms (shown in Fig. 3a), are in agreement with a azimuthal direction of the minimum compressive horizontal stress, $\sigma_3$, of approximately 260° (~~see~~ Fig. 7c). The lineaments of the geomorphological features, when compared to the focal mechanism results (~~see~~ Fig. 3a), also provide support for the notion that the fault associated to the largest shock has a strike of 174°, dip of 77° and rake of −85°. This fault and the average minimum compressive stress direction are consistent with the main trend of the southern extension of the BR province (Henry and Aranda-Gómez, 1992) much ~~in a similar fashion as~~ the Sanfandila sequence of 1998 (Zúñiga et al., 2003) ~~further~~ to the south. Thus, the PE~~s~~ yet additional evidence supporting the notion that the southern BR as an active region.





NHESSD
1, 323–352, 2013



CC BY

### 3.2 Seismic risk and hazard

The frequency of occurrence of large shallow earthquakes in the MVB zone is lower than those of the subduction zone. This situation and a low density of seismic instrumentation in the MVB (most of the stations are south of the MVB) have not allowed ~~to study~~ this type of shallow seismicity in detail. For example, at this moment it is not yet known: (1) what is the behavior of seismic attenuation from large shallow earthquakes within MVB, (2) what is the ground amplification level at different sites within the MVB, and (3) which buildings would ~~result~~ more affected, among ~~others.~~ These are some questions that must be answered with help of analysis such as the analysis presented here. Also, it is necessary to remember that the population ~~keeps~~ growing in this area ~~to a fastest~~ rate ~~than at other regions~~ in Mexico.

For the MVB zone, due to the short source distance of urban centers to the possible causative faults the risk posed by shallow local earthquakes is larger than the risk due to the subduction earthquakes. ~~This is due to its short source distances, in comparison to the subduction earthquakes.~~ The PGA amplitudes and their hypocentral distances ($R_h$) from this PES are presented in Fig. 8 and Table 7. In Table 7 it is possible see that the PGA on the Extoraz community site, where the EXT1 station was located, was close to 100 cm s$^{-2}$ at around $R_h$ = 6.0 km, due to the largest earthquake from PES of $M_w$ = 3.5. In contrast, the study of Clemente-Chavez et al. (2012) looking at subduction earthquakes showed a PGA = 0.12 cm s$^{-2}$, occurred at 27 April 2009 of $M_w$ = 5.6, with $R_h$ = 430.4 km, recorded at seismic station in Juriquilla, Queretaro; and more recently a PGA = 1.3 cm s$^{-2}$ was also recorded in Queretaro due to the Oaxaca earthquake occurred on 20 March 2012 of $M_w$ = 7.1. Regarding the site amplification level, if a 100 cm s$^{-2}$ PGA is contrasted with the PGA from vertical component ~~showed~~ in the Fig. 5, in general it can be estimated that there is a site amplification of around 4 times in the horizontal ground motion with respect to the vertical (PGA = 24 cm s$^{-2}$). Finally, in Fig. 6 is possible see the frequency range with the highest amplitudes, which ~~presents~~ low ~~frequencies,~~ between 0.5–6.0 Hz, this range can affect ~~to~~ buildings of up





NHESSD
1, 323–352, 2013



CC BY

to 20 levels, mainly. In general, these above comparisons show how the ground within the MVB can reach higher PGA, from small shallow earthquakes than the subduction earthquakes (except for Mexico City which is a well known special case).

Another aspect observed in one of the seismic records was the existence of premonitory earthquakes for the event No. 2 of Table 7 (see Fig. 9). These earthquakes occurred between 20 to 60 s before the main shock. When these premonitory earthquakes take place, it can be observed at short distances due to high signal/noise ratio. The importance of these earthquakes is the possibility to establish an early warning for this region.

## 4 Conclusions

From sequence of small earthquakes, which occurred, at the end of 2010 and beginning of 2011, near the town of Peñamiller, Queretaro, region that is located at the northeast border of the seismogenic zone known as the MVB where the seismicity activity is not common, but there are precedents of large earthquakes occurring in this zone (e.g. Suter et al., 1996), several important aspects were found:

1. The seismic location and source parameters were estimated through an inversion process and spectral analysis, whereby the largest earthquake had a moment magnitude of $M_w = 3.5$, that corresponds to a source area with a radius of 0.5 km, with a normal fault of strike of 174°, dip of 77° and rake of −85°. This earthquake occurred on 8 February 2011 at 19:53:48.6 UTC at latitude 21.039° and longitude −99.752° and at a 5.6 km depth. This place is located 7 km from downtown Peñamiller toward southeast, and at 3 km from the Extoraz community.

2. In general, all the earthquakes recordings correspond to normal faults. This, the lineaments of the geomorphological features, and the results of the statistical analysis of the $\sigma_1$ and $\sigma_3$ stress axes are congruent with the extensional regimen





NHESSD
1, 323–352, 2013



CC BY

with east-west direction ~~in~~ of the southern extension of the BR province. Furthermore, it is not far from the location of the largest historical event known to have occurred in the region (17 November 1887, mb ~ 5.3) which Suter et al. (1996) attribute to the same stress province.

3. Twenty-four good quality acceleration seismic records were registered by a temporary seismic network from the UAQ. Six records correspond to epicentral distances ~~minor to~~ 3.0 km, which are close to the seismic source of the largest event. With good quality records it is possible to see the P direct phase and to estimate *k* attenuation value, among other things.

4. Most of earthquakes ~~shown~~ here have acceleration levels greater that the acceleration values observed for subduction earthquakes ~~within of the~~ north MVB area ~~(up to 100 cm s$^{-2}$ of PGA)~~ ~~this~~ situation establish the necessity of further study of shallow earthquakes in central Mexico, since the hazard and risk posed by this type of events is very much neglected at this time.

~~This~~ paper ~~was~~ presented seismic information, which helps to gain more insight into the tectonic situation of the central Mexico region.

*Acknowledgements.* The authors are grateful to CONACYT for its support in this research. Alejandro Clemente Chavez wants to thank: CONACYT-Mexico for this funded support for his Ph-d studies under the project number 227579; to Gilberto Herrera Ruíz and Aurelio Domínguez González for their funded support in the installation of the temporary seismic network and its monitoring.

## References

Aguirre-Díaz, G. J., Nieto-Obregón, J., and Zúñiga, F. R.: Seismogenic basin and range and intra-arc normal faulting in the central Mexican Volcanic Belt, Queretaro, Mexico, Geol. J., 40, 215–243, doi:10.1002/gj.1004, 2005.

Alaniz-Álvarez, S. A. and Nieto-Samaniego, A. F.: El sistema de fallas Taxco-San Miguel de Allende y la Faja Volcánica Transmexicana, dos fronteras tectónicas del centro de México activas durante el Cenozoico, Boletín de la Sociedad Geológica Mexicana, 57, 63–80, 2005.
Alaniz-Álvarez, S. A., Nieto-Samaniego, A. F., and Ferrari, L.: Effect of the strain rate in the distribution of monogenetic and polygenetic volcanism in the Trans-Mexican volcanic belt, Geology, 26, 591–594, 1998.
Bouchon, M.: A simple method for calculating Green's functions for elastic layered media, Bull. Seism. Soc. Am., 71, 959–972, 1981.
Brune, J. N.: Tectonic stress and the spectra of seismic shear waves from earthquakes, J. Geophys. Res., 75, 4997–5009, 1970.
Clemente-Chavez, A., Arroyo, G., Moisés, Zúñiga Ramón, Figueroa Ángel, Pérez Miguel A., and López Carlos, S.: Relación de atenuación del movimiento del suelo para la aceleración máxima (PGA) sobre el Cinturón Volcánico Mexicano (MVB); análisis por trayectoria: Guerrero-Querétaro, Sociedad Mexicana de Ingeniería Sísmica, Revista de Ingeniería Sísmica, 87, 67–93, 2012.
Del Gaudio, V., Pierri, P., and Calcagnile, G.: Seismogenic zonation and seismic hazard estimates in a Southern Italy area (Northern Apulia) characterised by moderate seismicity rates, Nat. Hazards Earth Syst. Sci., 9, 161–174, doi:10.5194/nhess-9-161-2009, 2009.
Demant, A.: Características del Eje Neovolcánico Transmexicano y sus problemas de interpretación, Revista Instituto de Geología, Universidad Nacional Autónoma de México, 2, 172–187, 1978.
Demant, A.: Interpretación geodinámica del volcanismo del Eje Neovolcánico Transmexicano, Revista Instituto de Geología, Universidad Nacional Autónoma de México, 5, 217–222, 1981.
Ferrari, L., López-Martínez, M., González-Cervantes, N., Jacobo-Albarrán, J., and Hernández-Bernal, M. S.: Volcanic record and age of formation of the Mexico city basin, Unión Geofísica Mexicana, Resúmenes GEOS, 23(2), 120, ISSN 0186-1891, 2003.
Fuentes, C.: Inversión de la estructura cortical del sur de México utilizando velocidades de fase y grupo de ondas superficiales, Master Thesis, Instituto de Geofísica, UNAM, 1997.
García-Palomo, A., Macías, J., and Garduño, V.: Miocene to recent structural evolution of the Nevado de Toluca volcano region, Central Mexico, Tectonophysics, 318, 281–302, 2000.
Gómez-Tuena, A., Orozco-Esquivel, T., and Ferrari, L.: Petrogénesis ígnea de la faja volcánica transmexicana, Boletín de la Sociedad Geológica Mexicana, Vol. Conmemorativo del Centenario, Temas selectos de la Geología Mexicana, Tomo LVII, no. 3, 227–285, 2005.





NHESSD
1, 323–352, 2013

Havskov, J. and Ottemoller, L.: SEISAN: The earthquake analysis software, Institute of Solid Earth Physics, Norway, 2000.
Henry, C. D. and Aranda-Gómez, J. J.: The real southern Basin and Range: Mid- to Late cenozoic extension in Mexico, Geology, 20, 701–704, 1992.
Johnson, C. A. and Harrison, C. G. A.: Neotectonics in central Mexico, Phys. Earth Inter., 64, 187–210, 1990.
Kikuchi, M. and Kanamori, H.: Inversion of complex body waves – III, Bull. Seism. Soc. Am., 81, 2335–2350, 1991.
Martínez-Reyes, J. and Nieto-Samaniego, A. F.: Efectos geológicos de la tectónica reciente en la parte central de México, Revista Instituto de Geología, Universidad Nacional Autónoma de México, 9, 33–50, 1990.
Nieto-Samaniego, A. F., Ferrari, L., Alaniz-Alvarez, S. A., Labarthe-Hernández, G., and Rosas-Elguera, J.: Variation of Cenozoic extension and volcanism across the southern Sierra Madre Occidental Volcanic Province, Mexico, Geol. Soc. Am. Bull., 111, 347–363, 1999.
Nixon, G. T., Demant, A., Armstrong, R. L., and Harakal, J. E.: K-Arand geologic data bearing on the age and evolution of the Trans-Mexican Volcanic Belt, Geofís. Int., 26, 109–158, 1987.
Pasquaré, G., Ferrari, L., Perazzoli, V., Tiberi, M., and Turchetti, F.: Morphological and structural analysis of the central sector of the Transmexican Volcanic Belt, Geofís. Int., 26, 177–194, 1987.
Pasquaré, G., Garduño, V., Tibaldi, A., and Ferrari, M.: Stress pattern evolution in the central sector of the Mexican Volcanic Belt, Tectonophysics, 146, 353–364, 1988.
Polonia, A., Torelli, L., Gasperini, L., and Mussoni, P.: Active faults and historical earthquakes in the Messina Straits area (Ionian Sea), Nat. Hazards Earth Syst. Sci., 12, 2311–2328, doi:10.5194/nhess-12-2311-2012, 2012.
Rosas-Elguera, J. and Urrutia-Fucugauchi, J.: Tectonic control on the volcano-sedimentary sequence of the Chapala graben, western Mexico, Int. Geol. Rev., 40, 350–362, 1998.
Singh, S. K., Mena, E., Anderson, J. G., Quaas, R., and Lermo, J.: Source spectra and RMS accelerarion of Mexican Subduction zone earthquakes, PAGEOPH, 133, 477–474, 1990.
Singh, S. K., Iglesias, A., García, D., Pacheco, J. F., and Ordaz, M.: Q of Lg waves in the Central Mexican Volcanic Belt, Bull. Seism. Soc. Am., 97, 1259–1266, 2007.
Sokos, E. N. and Zahradnik, J.: ISOLA a Fortran code and a Matlab GUI to perform multiple-point source inversion of seismic data, Comput. Geosci., 8, 967–977, doi:10.1016/j.cageo.2007.07.005, 2008.





NHESSD
1, 323–352, 2013

Suter, M.: State of stress and active deformation in Mexico and western Central America in Decade of North American Geology, Neotectonics of North America, edited by: Slemmons, D. B., Engdahl, E. R., Zoback, M. D., and Blackwell, D. D., Geol. Soc. Am., Boulder, Colorado, Decade Map, 1, 401–421, 1991.

Suter, M., Carrillo, M., López, M., and Farrar, E.: The Aljibes halfgraben – active extension in the transition zone between the trans-Mexican volcanic belt and the southern Basin and Range, Mexico, Geol. Soc. Am. Bull., 107, 627–641, 1995.

Suter, M., Carrillo-Martínez, M., and Quintero-Legorreta, O.: Macroseismic study of shallow earthquakes in the central and eastern parts of the Trans-Mexican volcanic belt, Bull. Seism. Soc. Am., 86, 1952–1963, 1996.

Suter, M., López-Martínez, M., Quintero-Legorreta, O., and Carrillo-Martínez, M.: Quaternary intra-arc extension in the central Trans-Mexican volcanic belt, Geol. Soc. Am. Bull., 113, 693–703, 2001.

Urrutia-Fucugauchi, J. and Rosas-Elguera, J.: Paleomagnetic study of the eastern sector of 21 Chapala Lake and implications for the tectonics of west-central Mexico, Tectonophysics, 239, 61–71, 1994.

Vipin, K. S., Anbazhagan, P., and Sitharam, T. G.: Estimation of peak ground acceleration and spectral acceleration for South India with local site effects: probabilistic approach, Nat. Hazards Earth Syst. Sci., 9, 865–878, doi:10.5194/nhess-9-865-2009, 2009.

Zúñiga, F. R., Pacheco, J. F., Guzmán-Speziale, M., Aguirre-Díaz, G. J., Espíndola, V. H., and Nava, E.: The Sanfandila earthquake sequence of 1998, Queretaro, Mexico: activation of an undocumented fault in the northern edge of central Trans-Mexican Volcanic Belt, Tectonophysics, 361, 229–238, 2003.





NHESSD

1, 323–352, 2013



CC BY

**Table 1.** Events analyzed in this study: Peñamiller Earthquake Sequence (PES).

| Event No. | UTC Date (yyyy/mm/dd) | Number Records | Station Name |
|---|---|---|---|
| 1 | 2011/01/30 | 3 | EXT1, PIL1, HIG1 |
| 2 | 2011/01/30 | 3 | EXT1, PIL1, HIG1 |
| 3 | 2011/02/07 | 3 | EXT1, PIL1, HIG1 |
| 4 | 2011/02/07 | 3 | EXT1, PIL1, HIG1 |
| 5 | 2011/02/08 | 3 | EXT1, PIL1, HIG1 |
| 6 | 2011/03/01 | 3 | EXT1, PIL1, HIG2 |
| 7 | 2011/03/01 | 3 | EXT1, PIL1, HIG2 |
| 8 | 2011/03/26 | 3 | EXT1, PEN2, HIG2 |
| | | 24 | |





NHESSD
1, 323–352, 2013



CC BY

**Table 2.** Velocity structure used in the location and inversion procedures.

| Depth (km) | $V_p$ (km s$^{-1}$) | $V_s$ (km s$^{-1}$) |
|---|---|---|
| 0.0 | 4.15 | 2.40 |
| 2.2 | 5.06 | 2.92 |
| 5.2 | 6.10 | 3.52 |
| 7.0 | 6.29 | 3.63 |
| 20.3 | 7.45 | 4.30 |
| 99.0 | 8.04 | 4.64 |





NHESSD
1, 323–352, 2013

**Table 3.** Results of the locations of all events analyzed: Peñamiller Earthquake Sequence (PES).

| | | Origin time | Location | | | Error | | | rms |
|---|---|---|---|---|---|---|---|---|---|
| Event No. | UTC Date (yyyy/mm/dd) | UTC Hour (hh:mm:ss) | Lat. (°) | Long. (°) | *H* (km) | Lat. (km) | Long. (km) | *H* (km) | (s) |
| 1 | 2011/01/30 | 17:54:22.50 | 21.034 | −99.756 | 5.7 | 0.3 | 1.5 | 0 | 0.08 |
| 2 | 2011/01/30 | 17:54:41.70 | 21.034 | −99.756 | 5.6 | 0.3 | 1.5 | 0 | 0.08 |
| 3 | 2011/02/07 | 00:16:34.00 | 21.039 | −99.754 | 5.5 | 0.3 | 1.2 | 0 | 0.07 |
| 4 | 2011/02/07 | 09:42:54.50 | 21.024 | −99.725 | 2.0 | 0.6 | 1.6 | 2.0 | 0.08 |
| 5 | 2011/02/08 | 19:53:48.60 | 21.039 | −99.752 | 5.6 | 1.2 | 0.3 | 0 | 0.06 |
| 6 | 2011/03/01 | 12:59:40.70 | 21.031 | −99.759 | 6.1 | 0.3 | 2.1 | 0 | 0.09 |
| 7 | 2011/03/01 | 13:11:28.10 | 21.033 | −99.758 | 6.1 | 0.3 | 1.7 | 0 | 0.06 |
| 8 | 2011/03/26 | 01:42:17.40 | 21.015 | −99.806 | 4.3 | 0.5 | 0.8 | 1.5 | 0.03 |
| | | | | Averages | 5.11 | 0.48 | 1.34 | 0.44 | 0.07 |





NHESSD
1, 323–352, 2013



CC BY

**Table 4.** Earthquake source parameters of best fit solutions from the Peñamiller sequence.

| Event | UTC Date | Origin time | Location | | | Magnitude | Strike | Dip | Rake | Number |
|---|---|---|---|---|---|---|---|---|---|---|
| No. | (yyyy/mm/dd) | UTC Hour (hh:mm:ss) | Lat. (° N) | Long. (° W) | $H$ (km) | $M_w$ | $\phi$ (°) | $\delta$ (°) | $\lambda$ (°) | Records |
| 1 | 2011/01/30 | 17:54:22.50 | 21.034 | −99.756 | 5.7 | 2.1 | 154 | 61 | −116 | 3 |
| 2 | 2011/01/30 | 17:54:41.70 | 21.034 | −99.756 | 5.6 | 3.0 | 108 | 45 | −149 | 3 |
| 3 | 2011/02/07 | 00:16:34.00 | 21.039 | −99.754 | 5.5 | 2.9 | 41 | 57 | −162 | 3 |
| 4 | 2011/02/07 | 09:42:54.50 | 21.024 | −99.725 | 2.0 | 2.5 | 268 | 86 | −5 | 3 |
| 5 | 2011/02/08 | 19:53:48.60 | 21.039 | −99.752 | 5.6 | 3.5 | 174 | 77 | −85 | 3 |
| 6 | 2011/03/01 | 12:59:40.70 | 21.031 | −99.759 | 6.1 | 3.2 | 85 | 67 | −152 | 3 |
| 7 | 2011/03/01 | 13:11:28.10 | 21.033 | −99.758 | 6.1 | 2.7 | 133 | 64 | −143 | 3 |
| 8 | 2011/03/26 | 01:42:17.40 | 21.015 | −99.806 | 4.3 | 2.9 | 124 | 34 | −14 | 3 |
| | | | | | | Averages | 136 | 61 | −103 | |





NHESSD
1, 323–352, 2013



CC BY

**Table 5.** Results of spectral parameters from the largest earthquake in Peñamiller which occurred on 8 February 2011 at 19:53:48.60 UTC.

| Phase | $\Omega o$ (m s) | $f_o$ (Hz) | $a$ (m) | $\Delta\sigma$ (bar) | $M_o$ (N m) | $M_w$ |
|---|---|---|---|---|---|---|
| $P$ | $3.03 \times 10^{-6}$ | 6.0 | 516 | 5.1 | $1.59 \times 10^{14}$ | 3.4 |
| $S$ | $3.63 \times 10^{-6}$ | 5.8 | 228 | 11.1 | $3.02 \times 10^{13}$ | 2.9 |

$\Omega o$ = spectral flat level, $f_o$ = corner frequency, $a$ = source radius, $\Delta\sigma$ = static stress drop, $M_o$ = seismic moment and $M_w$ = magnitude moment.





NHESSD
1, 323–352, 2013

**Table 6.** Earthquake source parameters and values of the maximum ($\sigma_1$) and minimum ($\sigma_3$) compressive principal stresses axes from the PES.

| Event | UTC Date | Time origin | Magnitude | Strike | Dip | Rake | $\sigma_1$ | | $\sigma_3$ | |
|---|---|---|---|---|---|---|---|---|---|---|
| No. | (yyyy/mm/dd) | UTC Hour (hh:mm:ss) | $M_w$ | $\phi$ (°) | $\delta$ (°) | $\lambda$ (°) | Azimuth (°) | Plunge (°) | Azimuth (°) | Plunge (°) |
| 1 | 2011/01/30 | 17:54:22.50 | 2.1 | 154 | 61 | −116 | 19 | 63 | 263 | 13 |
| 2 | 2011/01/30 | 17:54:41.70 | 3.0 | 108 | 45 | −149 | 310 | 50 | 57 | 15 |
| 3 | 2011/02/07 | 00:16:34.00 | 2.9 | 41 | 57 | −162 | 257 | 35 | 355 | 12 |
| 4 | 2011/02/07 | 09:42:54.50 | 2.5 | 268 | 86 | −5 | 223 | 7 | 313 | 2 |
| 5 | 2011/02/08 | 19:53:48.60 | 3.5 | 174 | 77 | −85 | 90 | 58 | 261 | 32 |
| 6 | 2011/03/01 | 12:59:40.70 | 3.2 | 85 | 67 | −152 | 305 | 35 | 214 | 2 |
| 7 | 2011/03/01 | 13:11:28.10 | 2.7 | 133 | 64 | −143 | 352 | 44 | 257 | 5 |
| 8 | 2011/03/26 | 01:42:17.40 | 2.9 | 124 | 34 | −14 | 104 | 44 | 343 | 29 |
| | | | Averages | 136 | 61 | −103 | 208 | 42 | 258 | 14 |





NHESSD
1, 323–352, 2013



CC BY

**Table 7.** Amplitude of peak ground acceleration with respect to hypocentral distance from all events in each station.

| | Peak Ground Acceleration, PGA (cm s$^{-2}$)/Hypocentral distance $R_h$ (km) | | | | | | | | | | | | | | | |
|---|---|---|---|---|---|---|---|---|---|---|---|---|---|---|---|---|
| Station/Event No. [$M_w$] | 1 [2.1] | | 2 [3.0] | | 3 [2.9] | | 4 [2.5] | | 5 [3.5] | | 6 [3.2] | | 7 [2.7] | | 8 [2.9] | |
| EXT1 | 4.66 / | 6.11 | 27.23 / | 6.02 / | 9.28 / | 6.01 | 8.26 / | 5.93 | 93.63 / | 6.19 | 36.24 / | 6.41 | 7.82 / | 6.42 | 8.12 / | 5.74 |
| PIL1 | 4.95 / | 6.95 | 30.40 / | 6.86 / | 5.58 / | 6.59 | 4.42 / | 7.19 | 83.12 / | 6.74 | 16.81 / | 7.36 | 14.75 / | 7.28 | – | |
| HIG1 | 0.69 / | 13.92 | 1.91 / | 13.88 / | 0.50 / | 14.36 | 0.52 / | 12.39 | 3.44 / | 14.41 | – | | – | | – | |
| HIG2 | – | | – | | – | | – | | – | | 1.51 / | 13.68 | 0.38 / | 13.89 | 1.18 / | 11.87 |
| PEN2 | – | | – | | – | | – | | – | | – | | – | | 4.91 / | 6.14 |

PGA is root mean square of the horizontal components.





NHESSD
1, 323–352, 2013



CC BY

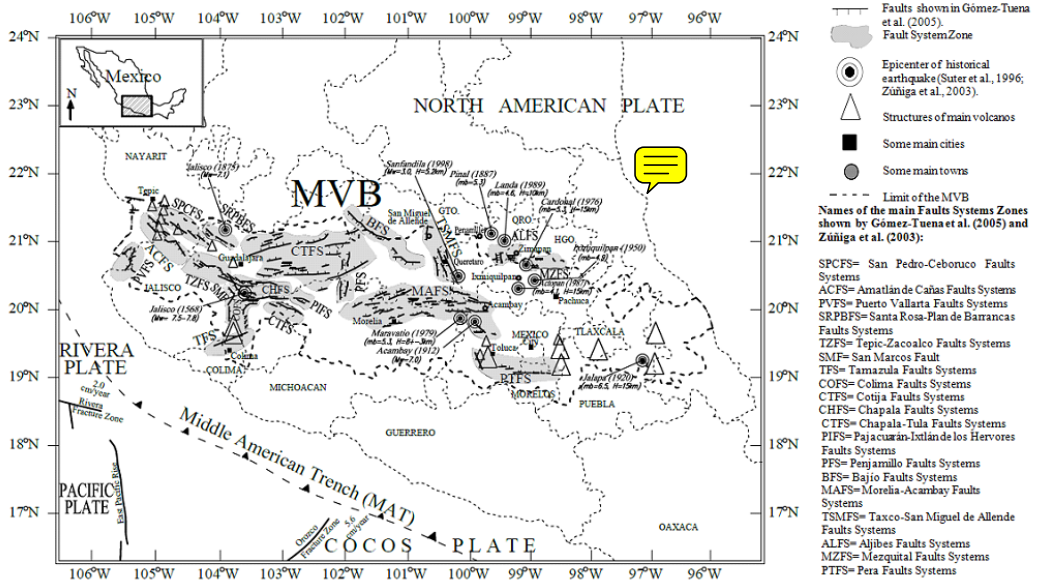


**Fig. 1.** Regional tectonic situation, main faults systems zones and historical large earthquakes of the MVB.





NHESSD
1, 323–352, 2013

Seismicity in northeast edge of the Mexican Volcanic Belt

A. Clemente-Chavez



CC BY

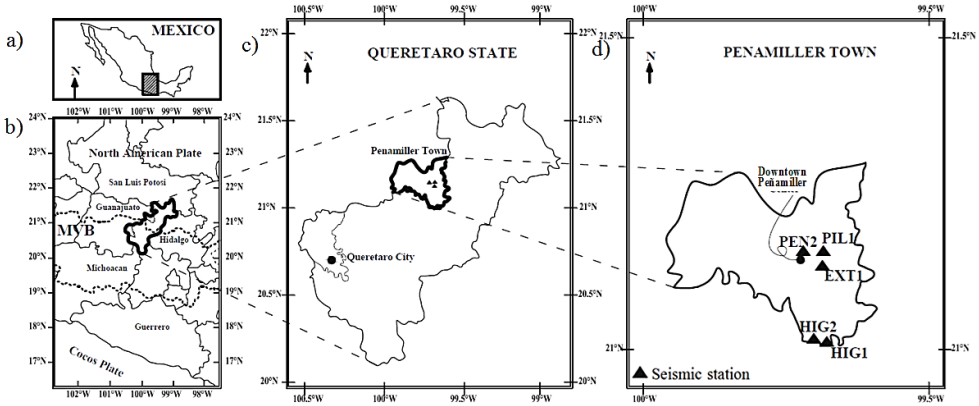


**Fig. 2.** The study area: northeast edge of the MVB. Location and identification of: **(a)** Mexico, **(b)** Queretaro state within Mexico and delimitation of MVB zone with dotted line, **(c)** Peñamiller Town and Queretaro City within Queretaro state, and **(d)** Seismic stations and Downtown Peñamiller.





NHESSD
1, 323–352, 2013



CC BY

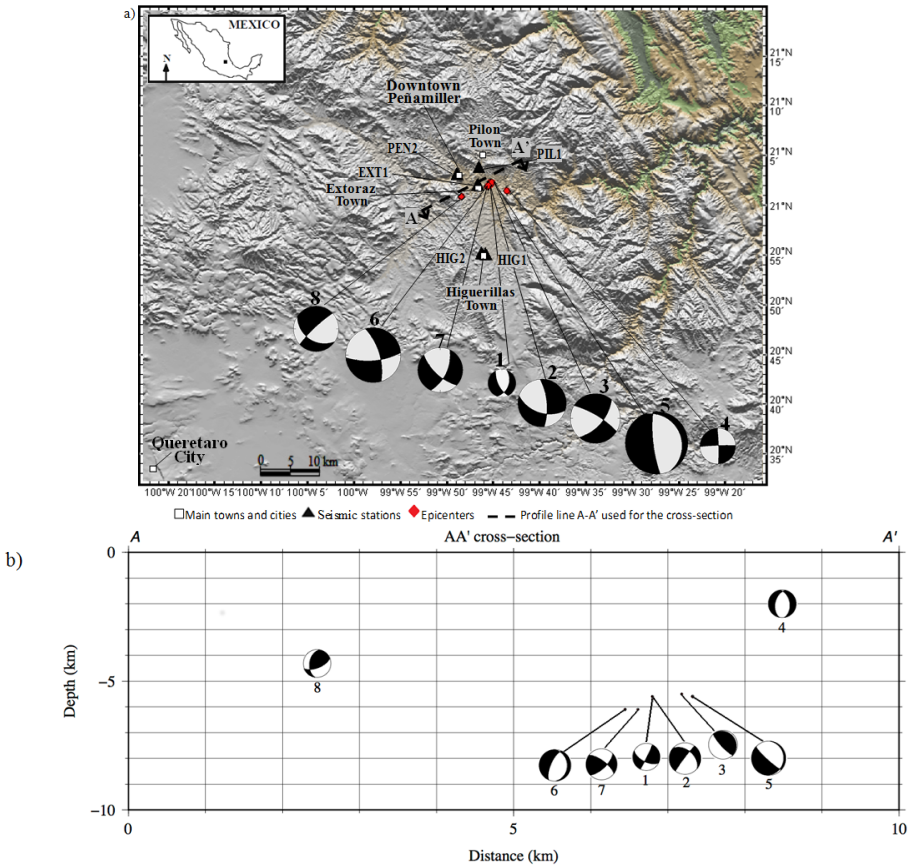


**Fig. 3. (a)** Epicenters of the Peñamiller Earthquakes Sequence and fault plane solutions (Focal Mechanisms) for eight events employed in the inversion procedure. **(b)** Cross-section $A - A'$ with hypocenters.





NHESSD
1, 323–352, 2013

Seismicity in northeast edge of the Mexican Volcanic Belt

A. Clemente-Chavez



CC BY

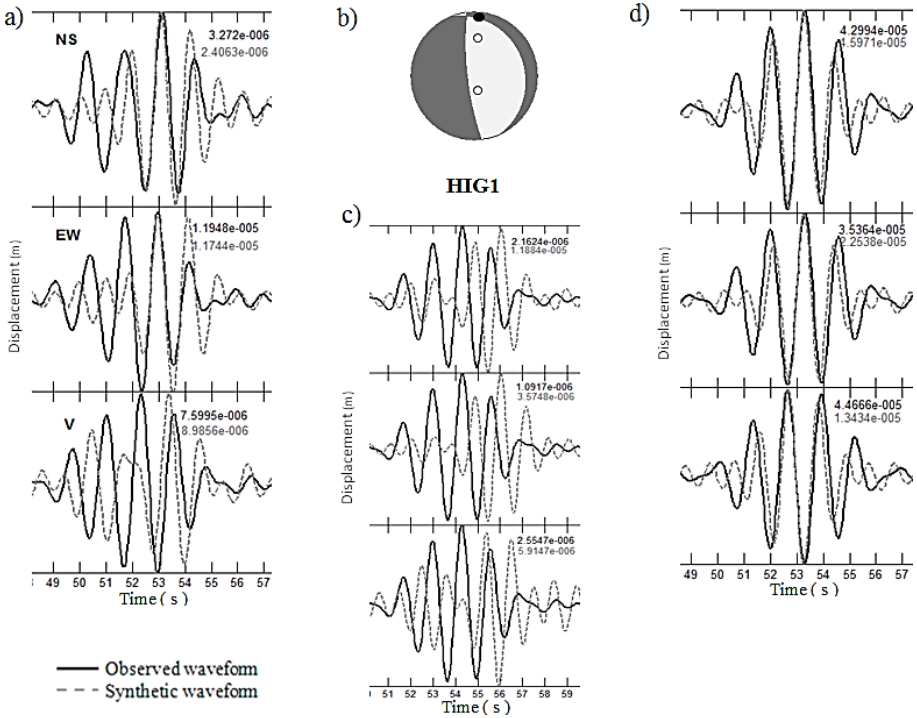


**Fig. 4. (a)**, **(c)** and **(d)** Observed and synthetic waveforms and their displacement amplitudes at each station for the largest earthquake $M_w = 3.5$ occurred on 8 February 2011 at 19:53:48.6 UTC. **(b)** Focal mechanism; first motion polarities are shown to compare with the best solution.





NHESSD
1, 323–352, 2013

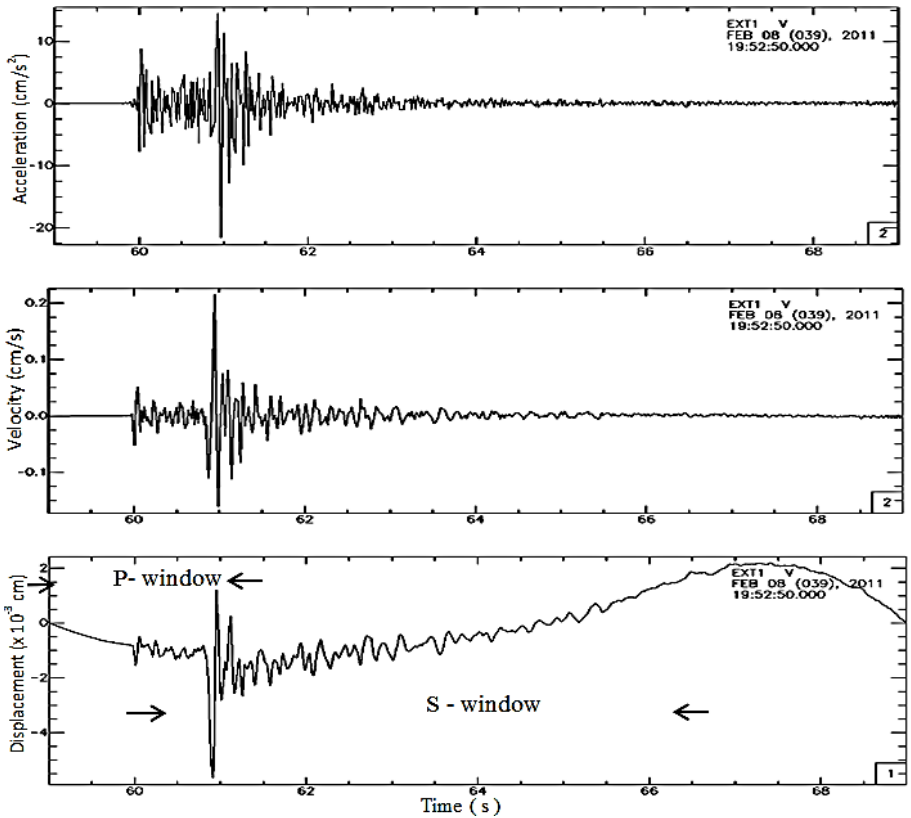


**Fig. 5.** Acceleration, velocity and displacement signal from the largest earthquake in Peñamiller that occurred on 8 February 2011 at 19:53:48.60 UTC are shown. Long of each phase-window on displacement signal for the spectral analysis are indicated with arrows. Note: Although P-window includes some of the *S* phase, this is eliminated by the taper which diminishes the effects of the window extremes.





NHESSD
1, 323–352, 2013

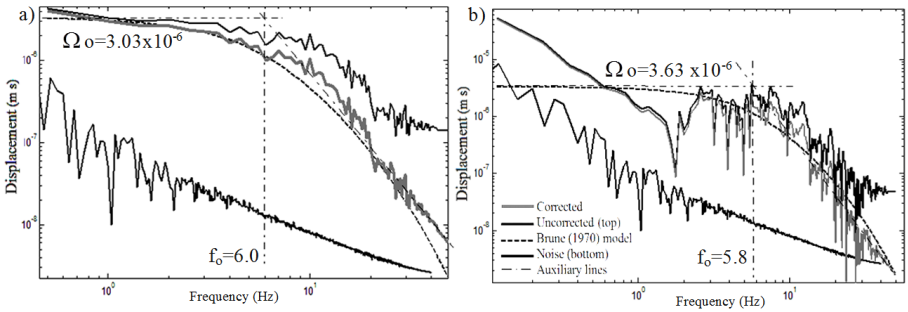


**Fig. 6. (a)** P-wave and **(b)** S-wave displacement spectrums from the largest earthquake in Peñamiller corrected and uncorrected for attenuation are shown. Spectral shape according to the Brune (1970) model and noise spectrum are also shown. The corner frequency $f_o$ and spectral flat level $\Omega o$ are identified.





NHESSD
1, 323–352, 2013

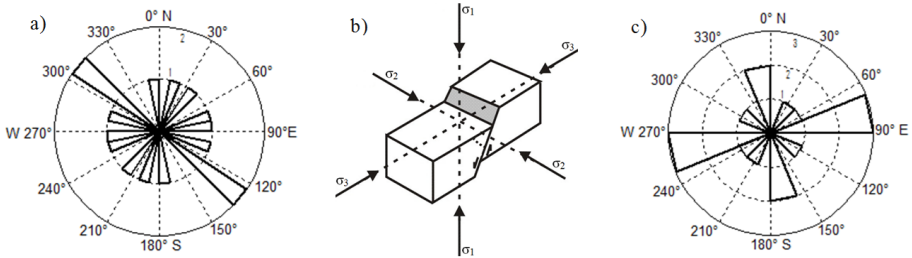


**Fig. 7.** Rose histograms: **(a)** Direction of maximum vertical ($\sigma_1$) and **(c)** minimum horizontal compressive stresses axes ($\sigma_3$). **(b)** A representation of the principal stress axes in a block-diagram of a normal fault.





NHESSD
1, 323–352, 2013

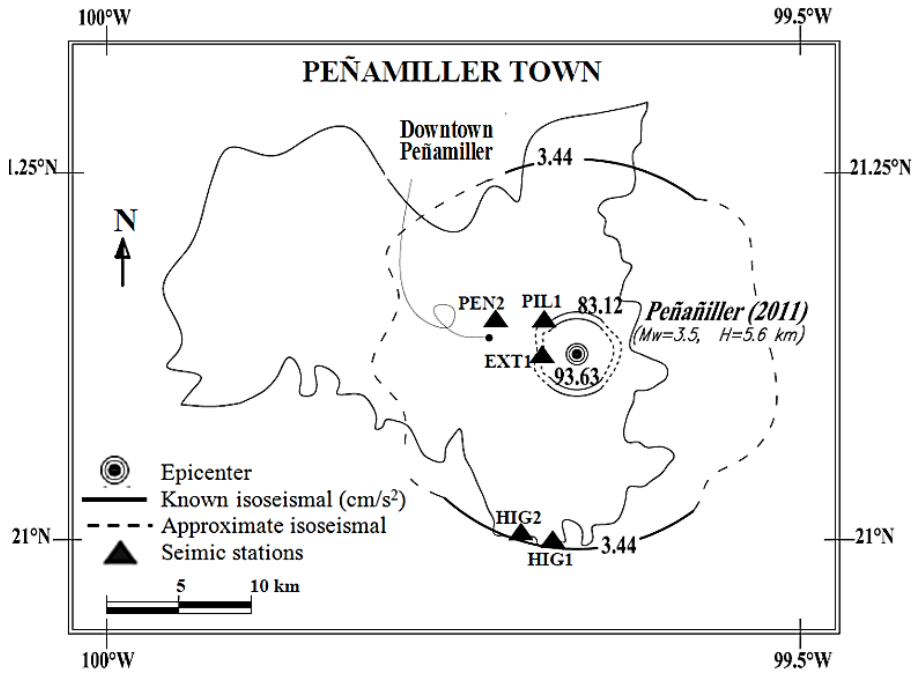


**Fig. 8.** Isoseismal of PGA amplitudes for the largest earthquake of $M_w$ = 3.5, seismic stations and downtown Peñamiller are shown.





NHESSD
1, 323–352, 2013

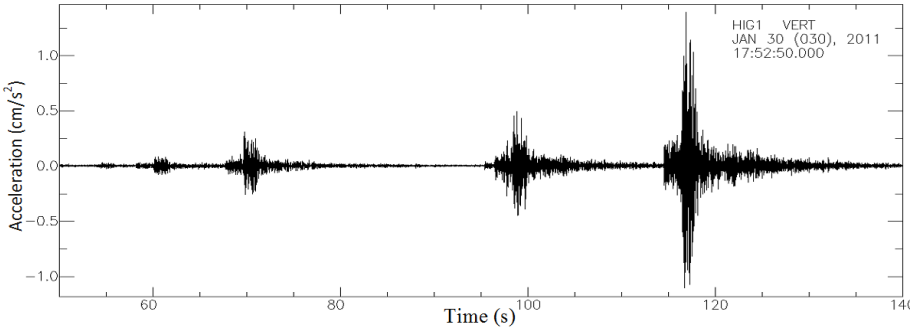


**Fig. 9.** Premonitory earthquakes for the event No. 2 of $M_w = 3.0$ are shown. In figure is observed that there are between 20 to 60 s before of the main shock.





NHESSD
1, 323–352, 2013